IEEE Photonics Journal
An IEEE Photonics Society Publication

Widely and Continuously Tunable Continuum Generation From CW-Pumped Cascaded Fibers

Volume 7, Number 4, August 2015

Chunyu Guo
Jun Yu
Shuangchen Ruan
Deqin Ouyang
Huaiqin Lin
Weiqi Liu
Yewang Chen
Peiguang Yan
Xuejuan Hu
Ping Hua

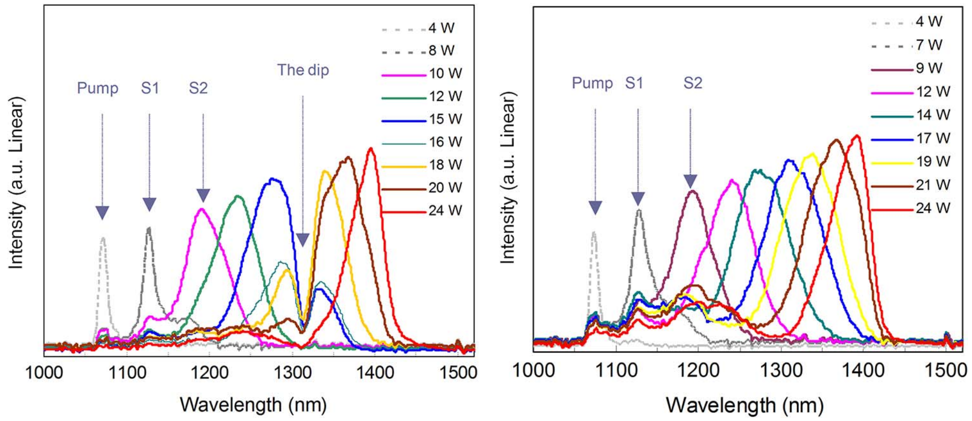

DOI: 10.1109/JPHOT.2015.2445091
1943-0655

Widely and Continuously Tunable Continuum Generation From CW-Pumped Cascaded Fibers

**Chunyu Guo,[1] Jun Yu,[1,2] Shuangchen Ruan,[1]
Deqin Ouyang,[1] Huaiqin Lin,[1] Weiqi Liu,[1,2] Yewang Chen,[1,2]
Peiguang Yan,[1] Xuejuan Hu,[1] and Ping Hua[1,3]**

[1]Shenzhen Key Laboratory of Laser Engineering, Key Laboratory of Advanced Optical Precision Manufacturing Technology of Guangdong Higher Education Institutes, College of Optoelectronic Engineering, Shenzhen University, Shenzhen 518060, China
[2]College of Electronic Science and Technology, Shenzhen University, Shenzhen 518060, China
[3]Optoelectronics Research Centre, University of Southampton, Southampton S09 5NH, U.K.

DOI: 10.1109/JPHOT.2015.2445091

Manuscript received April 6, 2015; revised June 8, 2015; accepted June 10, 2015. Date of current version June 19, 2015. This work was supported in part by the National Science Foundation of China under Grant 61308049 and Grant 61275144; by the Ph.D. Start-up Fund of the Natural Science Foundation of Guangdong Province under Grant S2013040012496; and by the Science and Technology Project of Shenzhen City under Grant JCYJ20120613110637373, Grant JCYJ20130329142022715, Grant JCYJ20140418091413568, and Grant JCYJ20130329103213543. Corresponding author: S. Ruan (e-mail: scruan@szu.edu.cn).

Abstract: A tunable continuum with multiwatt output power is demonstrated for the first time through the pumping of cascaded fibers by using a continuous-wave (CW) ytterbium fiber laser. The central wavelength of the output continuum can be tuned continuously and monotonically by varying input pump power, with a wide wavelength-tunable range from 1.2 to 1.4 μm and a 3-dB bandwidth of tens of nanometers. Two configurations of the cascaded fibers both display the power-dependent wavelength tunability. The output spectral characteristics are presented, and the generation of the CW-pumped tunable continuum is tentatively attributed to the seed-dependent Raman amplification.

Index Terms: Wavelength-tunable optical source, supercontinuum (SC), photonic crystal fiber (PCF), stimulated Raman scattering (SRS).

1. Introduction

Widely wavelength-tunable optical sources have always been an attractive research field for their wavelength-tunable properties [1]–[5]. Since the discovery of the soliton self-frequency shift (SSFS), wavelength-tunable optical sources have been developed extensively because of their unique power-dependent wavelength tunability. With the pumping of a special fiber by using a fixed-wavelength ultrashort pulse laser, SSFS can be used to achieve a widely tunable optical source at different wavelength ranges by varying the input power. As fiber input power is increased, the wavelengths of generated soliton pulse are red-shifted continuously and monotonically. Aside from input power, this wavelength shift increases with fiber length. Nishizawa and Goto developed 1.56 μm to 1.78 μm widely wavelength-tunable output which employed a 180 fs passively mode-locked Er-doped femtosecond fiber laser and polarization-maintaining fibers [6]. Through a 66 fs Yb-doped ultrashort pulse fiber laser and a photonic crystal fiber (PCF), a

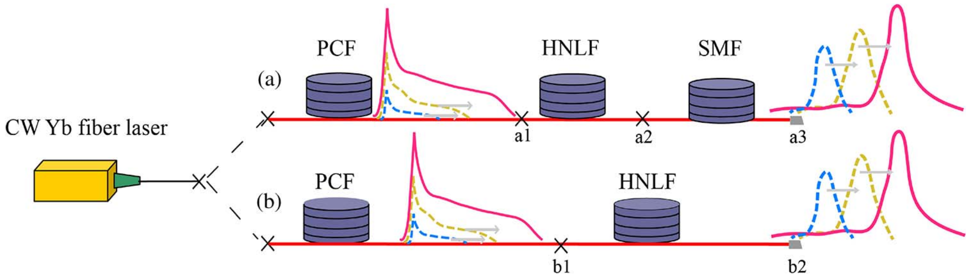

Fig. 1. Experimental setup for tunable continuum generation. The points of a1, a2, and a3 represent the end points from PCF250, PCF250-HNLF90, and PCF250-HNLF90-SMF8K in configuration (a). The points of b1 and b2 represent the end points from PCF250 and PCF250-HNLF in configuration (b).

wavelength-tunable soliton pulse source of 1.06 μm to 1.68 μm was generated [7]. Moreover, wavelength-tunable optical sources could be developed in other fiber platforms, including hollow-core photonic bandgap fibers [8], solid silica higher order mode fibers [9] and large-mode-area fibers [10].

Despite extensive developments, the primary pump sources for these SSFS-based wavelength-tunable optical sources are the ultrashort pulse lasers with high complexity, and the generated tunable output is at the mW-level average power, which limits some applications of these tunable sources. As far as we know, high-power widely and continuously tunable optical sources have not been previously demonstrated. It is known to all that SSFS could also be a principal mechanism for high-power, wideband, Raman-soliton supercontinuum (SC) generation with the high-power pumping of a dispersion-optimized, highly nonlinear PCF [11]–[19]. The tunable output also could be realized through the tunable filtering for the wideband SC [20], [21]. However, this wavelength-tunability is based on the loss on the undesirable wavelength range of the SC. Therefore, the question that needs to be addressed is whether the SSFS-based, high-power, wideband, Raman-soliton SC could be directly converted to the widely and continuously tunable output without the loss on other wavelength range.

In a previous paper, we demonstrated a spectrum-flattening approach for a continuous wave (CW) supercontinuum through fiber cascading [22]. In the present study, we developed a high-power widely and continuously tunable continuum source from a CW-pumped wideband SC through fiber cascading. The wavelength tunability is demonstrated in two configurations of cascaded fiber: a three-cascaded fiber of photonic-crystal fiber (PCF)/highly nonlinear fiber (HNLF)/single-mode optical fiber (SMF) and a two-cascaded fiber of PCF/HNLF. The mechanism of CW-pumped wavelength tunability is discussed basing on the spectral characteristics of the output.

2. Experimental Setup

Fig. 1 shows the experimental setup. The pump was a 24 W single-mode, randomly polarized, CW Yb-fiber laser at 1071.5 nm with a line width of 0.5 nm. This laser pumped two fiber configurations with different kinds of cascaded fibers. The output ends of the cascaded fibers were angle-cleaved to reduce reflection from the end facet. The output power and spectrum were directly monitored by using a thermal power meter (Spectrum Physics, 407 A) and an optical spectrum analyzer (StellarNet, EPP 2000, 900 nm to 1700 nm).

Three fibers were used in our experiment: a highly nonlinear PCF, a normal-dispersion HNLF, and a standard SMF. The PCF, which was previously used for CW supercontinuum generation, has a single zero-dispersion wavelength (ZDW) of 1030 nm with a nonlinear coefficient of $11\ (\mathrm{W}\cdot\mathrm{km})-1$ and a mode field diameter of 3.9 μm. The HNLF, which was previously used for supercontinuum flattening, has the nonlinear and Raman gain coefficients of $10\ (\mathrm{W}\cdot\mathrm{km})-1$ and $4.8\ (\mathrm{W}\cdot\mathrm{km})-1$, respectively, at 1550 nm [22]. The ZDW (1840 nm) of this HNLF is sufficiently large, which guarantees that all the spectral components of input lie in the normal dispersion region. The SMF is a standard communication single-mode fiber with a ZDW of 1310 nm.

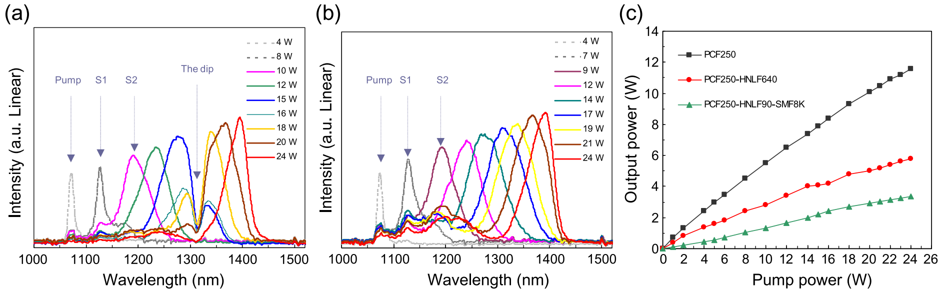

Fig. 2. Spectrum evolutions of the output tunable continuum with increasing pump power from (a) PCF250-HNLF90-SMF8K and (b) PCF250-HNLF640. Powers marked represent the pump powers. (c) Output powers versus pump power from PCF250-HNLF90-SMF8K, PCF250-HNLF640, and PCF250. The output powers of the tunable continua from PCF250-HNLF90-SMF8K and PCF250-HNLF640 range 1.3 W $\sim$ 3.3 W and 2.8 W $\sim$ 5.8 W, respectively, corresponding to the pump from 10 W to 24 W.

Configuration (a) has three kinds of fibers cascaded: a 250 m PCF, a 90 m HNLF, and an 8 km SMF (PCF250-HNLF90-SMF8K). The pump fiber laser was directly spliced to the PCF with a splice loss of 0.5 dB. The 90 m HNLF was cascaded with the PCF with a splice loss of 0.4 dB. The SMF was spliced to the HNLF with a 0.3 dB loss. Configuration (b) has two kinds of fibers cascaded: a 250 m PCF and the HNLF with different lengths (PCF250-HNLF).

3. Experimental Results

3.1. Three-Cascaded Fiber Configuration

Fig. 2(a) shows the output spectra from the three-cascaded fiber of PCF250-HNLF90-SMF8K with increasing pump power. The pump laser was transferred to the first-order Raman Stokes peak line (S1) at 1127 nm and then to the second-order Raman Stokes peak line (S2) at 1190 nm. The spectral width centered at S2 was further broadened to 62 nm, forming a continuum. Afterward, the continuum was kept shifting monotonically toward longer wavelengths until $\sim$1400 nm at the maximum pump power, just with a dip occurring at 1310 nm in the wavelength-shifting process. When the continuous wavelength shift reached 1290 nm, the continuum did not shift continuously with increasing pump power but changed to 1340 nm across 1310 nm, thereby forming the dip. The output power from the three-cascaded fiber increased with pump power is shown in Fig. 2(c), and the wavelength-tunable output had a maximum power of 3.4 W at 1397 nm with a bandwidth of 47 nm. The ratio of the power around the longest peak wavelength (1390 nm) to the total output power was measured to be 72%.

Output spectrum evolutions from different points of PCF250-HNLF90-SMF8K are compared in Fig. 3. The pumping of a long-length PCF by using a CW Yb fiber laser generated a supercontinuum (SC) originated from the modulation instability (MI)-induced SSFS [12]–[14]; the cascading of an optimal length of HNLF with the PCF demonstrated spectrum flattening for a supercontinuum [22]; and the cascading of a long SMF with the HNLF achieved a tunable continuum.

3.2. Two-Cascaded Fiber Configuration

We cascaded only different lengths of HNLF with the 250 m PCF for comparison to analyze the effect of HNLF on wavelength-tunable continuum generation. Fig. 4 shows output spectrum evolutions with pump power from the cascaded fibers of PCF250-HNLF320, PCF250-HNLF480, and PCF250-HNLF640.

If the HNLF was short, with increased pump power, the pump spectrum broadened to longer wavelengths, forming a continuum, and a portion of pump energy was transferred to S1 and then to S2 to obtain a flatter spectrum, as shown in Figs. 3(b) and 4(a). However, if the HNLF was long enough (as in PCF250-HNLF640), output spectrum evolution was different in Fig. 4(c).

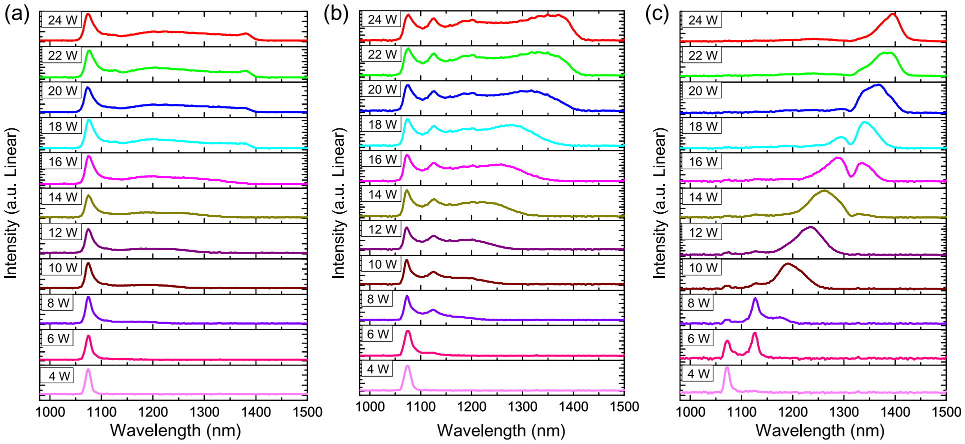

Fig. 3. Output spectrum evolutions with pump power at three end points of PCF250-HNLF90-SMF8K in Fig. 1(a). (a) At a1 point. (b) At a2 point. (c) At a3 point. Powers marked represent the pump powers.

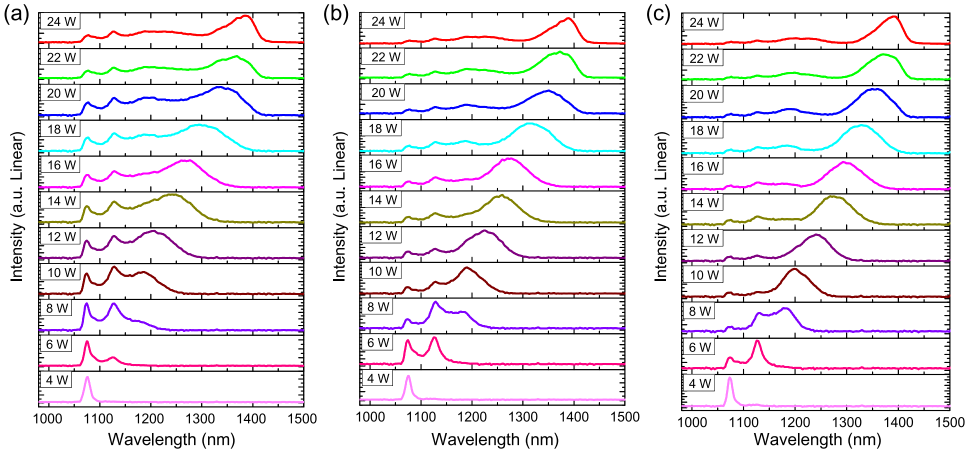

Fig. 4. Output spectrum evolutions with pump power from the cascaded fiber of PCF250-HNLF in Fig 1(b). (a) From PCF250-HNLF320. (b) From PCF250-HNLF480. (c) From PCF250-HNLF640. HNLF320: a 320 m HNLF; HNLF480: a 480 m HNLF; HNLF640: a 640 m HNLF.

Most energy of the pump and the first-order Stokes laser were both transferred to S2, broadening to a continuum centered at this wavelength. Then, the continuum shifted continuously to longer wavelengths just as the spectrum evolved from the three-cascaded fiber configuration. The spectral dip at 1310 nm from the three-cascaded fiber configuration disappeared in the two-cascaded fiber configuration. Finally, the widely and continuously tunable continuum was achieved, which has a wavelength-tunable range of 200 nm (1190 nm to 1394 nm), a 3 dB bandwidth of 58 nm to 88 nm, and an output power of 2.8 W to 5.8 W in Fig. 2(b) and (c). And the ratio of the power around the longest peak wavelength (1390 nm) to the total output power was measured to be 65%.

3.3. Output Spectral Characteristics

Fig. 5 shows the spectral characteristics of the output from different cascaded fibers. The central wavelengths of the continua varied monotonically with pump power, close to the supercontinuum long-wavelength edge (SC-LWE). In the same kind of fiber configuration pumped with constant power, a longer cascaded fiber corresponded to a narrower bandwidth and a slightly longer central wavelength closer to the SC-LWE. Central wavelengths from the cascaded fibers

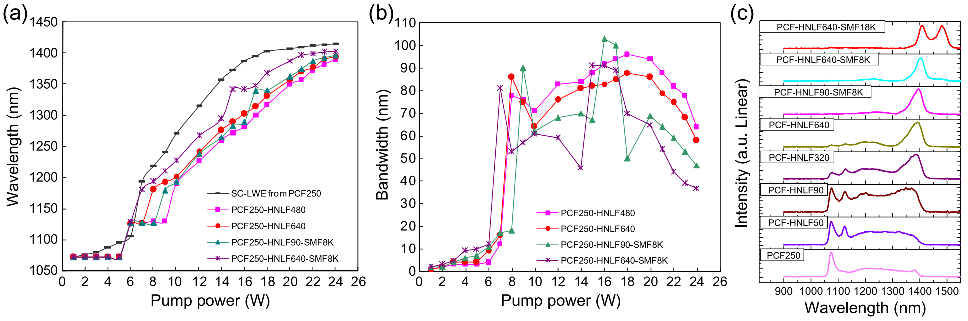

Fig. 5. Output spectral characteristics from different fiber configurations. (a) Central wavelengths from four kinds of cascaded fibers and the SC-LWEs from PCF250 versus pump powers. SC-LWE: supercontinuum long-wavelength edge of 15 dB. (b) Output 3 dB bandwidths versus pump powers. Another three-cascaded fiber of PCF250-HNLF640-SMF8K was also tested, and the output spectrum evolution was similar with that from PCF250-HNLF90-SMF8K, only with a much lower output power. (c) Output spectra at the maximum pump power of 24 W. SMF18K: an 18 km SMF; PCF: PCF250.

of PCF250-HNLF480, PCF250-HNLF640, PCF250-HNLF90-SMF8K, and PCF250-HNLF640-SMF8K with the pump power of 24 W were 1390, 1394, 1397, and 1404 nm (long-wavelength edge from PCF250 was 1415 nm), with bandwidths of 64, 58, 47, and 37 nm, respectively.

When the pump power exceeded 20 W, the bandwidth of the continuum decreased, and the central wavelength extended slowly, corresponding to the slow extension of the SC-LWE in this pump range. Provided that the cascaded fiber was long enough (PCF250-HNLF640-SMF18K), after moving to 1400 nm, the continuum spectrally narrowed and did not shift continuously with further increases in pump power and instead transferred to its Stokes line of 1480 nm in Fig. 5(c).

Break points with pump power of 6 W to 10 W both in Fig. 5(a) and (b) represented the energy transferring process from the first-order Raman laser to the continuum. Greater length in a configuration caused this energy transfer occurring at a lower pump level. Whereas break points from 14 W to 18 W in the three-cascaded fiber configuration represented the energy transfer across the spectrum dip at 1310 nm.

4. Discussion

As already noted, the wavelength tunability of the output continuum from the CW pump was similar with the wideband and continuous wavelength tunability of the SSFS-based soliton pulse sources from the ultrashort pulse pump [6], [7]. According to the output spectrum evolutions in the two-cascaded fiber configuration in Fig. 4, the Raman effect was significant to the formation and shifting of the continuum. With the increase of pump power, the pump energy was transferred to S1 and then to S2 based on the cascaded stimulated Raman scattering (SRS) in the normal-dispersion HNLF. And with the propagation along the cascaded HNLF, more short-wavelength energy was transferred to the shifting continuum. However, after formed around S2, the continuum shifted to longer wavelengths with increasing pump power, which did not result only from the cascaded SRS of the pump. Moreover, the SSFS could not exist in the normal-dispersion fiber to result in the wavelength shift of the continuum [23], [24].

Here, we tentatively attribute the generation of the wavelength-tunable continuum to the seed-dependent Raman amplification that is the Raman amplification of the long wavelength-extending seed. The Raman amplification occurred in the cascaded HNLF section, and the injected seed is the SSFS-based long wavelength-extending SC from the preceding PCF section. At the initial stage of increasing the pump power, the remaining pump field in the HNLF amplified the injected SC spectral components within the Raman gain band through SRS, thereby forming a continuum around the Stokes line. With the further increase of pump power, the SSFS-based longer-wavelength SC spectral components are continuously generated in the PCF. When the longer-wavelength SC components were continuously injected into the HNLF, these long-wavelength seeds could be Raman-amplified continuously by the short-wavelength components of the formed continuum, with the short-wavelength components consumed constantly. Accordingly, similar to the SSFS based on intra-pulse Raman scattering, the general wavelengths of the continuum shift continuously toward longer wavelengths.

According to this interpretation, the reason why the continuum began to form at S2 and not at S1 can be deduced from Fig. 5(a). Even at a pump level of 6 W, at which S1 was generated in the cascaded HNLF [see also Fig. 4(c)], the SC from the PCF had still not broadened to this wavelength [see also Fig. 3(a)], which indicates that no spectral components at S1 could be injected into the HNLF and amplified by SRS. The SC then extended rapidly across S1 to S2 with further increases in pump power, and spectral components around the second-order Raman gain region were Raman-amplified to a continuum.

After the wavelength shift of the continuum was achieved through the Raman amplification of the continuously-injected longer-wavelength components, the wavelength-shifting range can be determined by the longest wavelength of the SC from the PCF. Therefore, unlike in SSFS, the length of cascaded HNLF was of secondary importance to the wavelength-shifting range of the continuum; however, SC-LWE had a more significant effect. Longer HNLF with higher Raman gain merely resulted in more short-wavelength components transferred to long-wavelength components. Accordingly, the spectral width of the continuum narrowed as the central wavelength shifted a little in Fig. 5(a) and (b).

However, if the cascaded fiber was sufficiently long to shift the central wavelength of the continuum to the SC-LWE, the continuum would not shift continuously to longer wavelengths because of the lack of longer-wavelength seeds but would be transferred to the Raman Stokes line of the narrower continuum through SRS [see the results from PCF-HNLF640-SMF18K in Fig. 5(c)].

In the three-cascaded fiber configuration, it is thought to be the high nonlinearity from the combination of tens of meters of HNLFs and thousands of meters of SMFs that gave rise to Raman amplification of the longer-wavelength seeds, thereby forming the wavelength-tunable continuum. The dip at 1310 nm in the wavelength-shifting process from this fiber configuration is attributed to the spectral splitting of the injected SSFS-induced SC spectral components at the ZDW of the SMF [25].

5. Conclusion

We have demonstrated a high-power widely and continuously wavelength-tunable continuum from 1.2 μm to 1.4 μm through a CW-pumped cascaded fiber configuration. The output spectral characteristics of the tunable continuum were analyzed by comparing spectrum evolutions from the different configurations and lengths of cascaded fibers. Generation of the wavelength-tunable continuum was discussed and tentatively attributed to the seed-dependent Raman amplification. This wavelength-tunable continuum source should be promising for a variety of applications, such as the multi-wavelength lidar system, atmospheric constituent measurement, remote sensing, and optical coherence tomography.

References

[1] N. Nishizawa, “Highly functional all-optical control using ultrafast nonlinear effects in optical fibers,” *IEEE J. Quantum Electron.*, vol. 45, no. 11, pp. 1446–1455, Nov. 2009.

[2] E. R. Andresen, V. Birkedal, J. Thøgersen, and S. R. Keiding, “Tunable light source for coherent anti-Stokes Raman scattering microspectroscopy based on the soliton self-frequency shift,” *Opt. Lett.*, vol. 31, no. 9, pp. 1328–1330, Jan. 2006.

[3] A. Kudlinski, A. Mussot, R. Habert, and T. Sylvestre, “Widely tunable parametric amplification and pulse train generation by heating a photonic crystal fiber,” *IEEE J. Quantum Electron.*, vol. 47, no. 12, pp. 1514–1518, Dec. 2011.

[4] S. A. Dekker *et al.*, “Highly-efficient, octave spanning soliton self-frequency shift using a specialized photonic crystal fiber with low OH loss,” *Opt. Exp.*, vol. 19, no. 18, pp. 17 766–17 773, Aug. 2011.

[5] J. Lee, J. van Howe, C. Xu, and X. Liu, “Soliton self-frequency shift: Experimental demonstrations and applications,” *IEEE J. Sel. Top. Quantum Electron.*, vol. 14, no. 3, pp. 713–723, Jun. 2008.

[6] N. Nishizawa and T. Goto, “Compact system of wavelength-tunable femtosecond soliton pulse generation using optical fibers,” *IEEE Photon. Technol. Lett.*, vol. 11, no. 3, pp. 325–327, Mar. 1999.

[7] J. Takayanagi, T. Sugiura, M. Yoshida, and N. Nishizawa, “1.0–1.7 μm wavelength-tunable ultrashort-pulse generation using femtosecond Yb-doped fiber laser and photonic crystal fiber,” *IEEE Photon. Technol. Lett.*, vol. 18, no. 21, pp. 2284–2286, Nov. 2006.

[8] D. G. Ouzounov *et al.*, “Generation of megawatt optical solitons in hollow-core photonic band-gap fibers,” *Science*, vol. 301, no. 5640, pp. 1702–1704, Sep. 2003.

[9] J. van Howe *et al.*, “Demonstration of soliton self-frequency shift below 1300 nm in higher-order mode, solid silica-based fiber,” *Opt. Lett.*, vol. 32, no. 4, pp. 340–342, Jan. 2007.

[10] K. Wang and C. Xu, “Wavelength-tunable high-energy soliton pulse generation from a large-mode-area fiber pumped by a time-lens source,” *Opt. Lett.*, vol. 36, no. 6, pp. 942–944, Mar. 2011.

[11] J. M. Dudley and J. R. Taylor, “Ten years of nonlinear optics in photonic crystal fibre,” *Nat. Photon.*, vol. 3, pp. 85–90, Feb. 2009.

[12] J. M. Dudley, G. Genty, and S. Coen, “Supercontinuum generation in photonic crystal fiber,” *Rev. Mod. Phys.*, vol. 78, no. 4, pp. 1135–1184, Oct. 2006.

[13] J. C. Travers, A. B. Rulkov, B. A. Cumberland, S. V. Popov, and J. R. Taylor, “Visible supercontinuum generation in photonic crystal fibers with a 400W continuous wave fiber laser,” *Opt. Exp.*, vol. 16, no. 19, pp. 14 435–14 447, Aug. 2008.

[14] A. Kudlinski and A. Mussot, “Visible cw-pumped supercontinuum,” *Opt. Lett.*, vol. 33, no. 20, pp. 2407–2409, Oct. 2008.

[15] A. Kudlinski *et al.*, “White-light cw-pumped supercontinuum generation in highly GeO2-doped-core photonic crystal fibers,” *Opt. Lett.*, vol. 34, no. 23, pp. 3631–3633, Nov. 2009.

[16] D. Labat *et al.*, “Phosphorus-doped photonic crystal fibers for high-power (36 W) visible CW supercontinuum,” *IEEE Photon. J.*, vol. 3, no. 5, pp. 815–820, Oct. 2011.

[17] H. F. Wei *et al.*, “A compact seven-core photonic crystal fiber supercontinuum source with 42.3 W output power,” *Laser Phys. Lett.*, vol. 10, no. 4, Apr. 2013, Art. ID. 045101.

[18] H. W. Chen, Z. L. Chen, S. P. Chen, J. Hou, and Q. S. Lu, “Hundred-watt-level, all-fiber-integrated supercontinuum generation from photonic crystal fiber,” *Appl. Phys. Exp.*, vol. 6, no. 3, Mar. 2013, Art. ID. 032702.

[19] S. P. Chen *et al.*, “20 W all fiber supercontinuum generation from picosecond MOPA pumped photonic crystal fiber,” *Laser Phys.*, vol. 21, no. 3, pp. 519–521, Feb. 2011.

[20] K. F. Mak, J. C. Travers, P. Hölzer, N. Y. Joly and P. S. J. Russell, “Tunable vacuum-UV to visible ultrafast pulse source based on gas-filled Kagome-PCF,” *Opt. Exp.*, vol. 21, no. 9, pp. 10 942–10 953, Apr. 2013.

[21] SuperK VARIA-Variable Bandpass Filter: Turn Your Supercontinuum Source Into a High Power Tunable Laser. [Online]. Available: http://www.nktphotonics.com/superk_varia?cid=7913

[22] C. Guo, S. Ruan, P. Yan, E. Pan, and H. Wei, “Flat supercontinuum generation in cascaded fibers pumped by a continuous wave laser,” *Opt. Exp.*, vol. 18, no. 11, pp. 11 046–11 051, May 2010.

[23] G. P. Agrawal, *Nonlinear Fiber Optics*, 4th ed. Boston, MA, USA: Academic, 2007.

[24] J. Dudley and J. Taylor, *Supercontinuum Generation in Optical Fibers*. Cambridge, U.K.: Cambridge Univ. Press, 2010.

[25] A. Gouveia-Neto, M. E. Faldon, and J. R. Taylor, “Solitons in the region of the minimum group-velocity dispersion of single-mode optical fibers,” *Opt. Lett.*, vol. 13, no. 9, pp. 770–772, Sep. 1988.